COBEM 2023 27TH INTERNATIONAL CONGRESS OF MECHANICAL ENGENEERING

ABCM Brazilian Society of Mechanical Sciences and Engineering
27th ABCM International Congress of Mechanical Engineering
December 04-08, 2023, Florianópolis-SC, Brazil

Modelling and Control of a Passenger Vehicle with an Active Anti-Roll Bar

Éverton L. de Oliveira[1]
Andrei A. Felix[1]
Diego Cólon[1]
ev_lins@usp.br, andreifelix@usp.br, diego@lac.usp.br,
[1]Lab. of Control and Automation (LCA), Telecommunications and Control Engineering Depart., University of São Paulo (USP)
CEP: 05508-010, São Paulo – SP, Brazil
Fernando Malvezzi[2]
fernando.malvezzi@maua.br
[2]Mechanical Engineering Depart., Mauá Institute of Technology
CEP: 09580-900, São Caetano do Sul – SP, Brazil
Tarcisio Hess-Coelho[3]
tarchess@usp.br
[3]Lab. of Mechanisms, Machines and Robots (LaMMaR), Mechatronics and Mechanical Systems Engineering Depart., Escola Politecnica, University of São Paulo (USP)
CEP: 05508-030, São Paulo – SP, Brazil

Abstract. *During the last decades, traffic safety has become a major concern in nowadays society. In fact, due to traffic road crashes, a significant number of people either get severely injured or die yearly. As a consequence, many countries have changed their legislation in order to demand that manufactured vehicles conform to impact regulations and incorporate any kind of active chassis system. Such technologically advanced machines must not only be safe but also effective and efficient, which will demand to include even more sophisticated active chassis systems. In this context, the current paper presents the modelling and control of a passenger vehicle equipped with an active anti-roll bar. Initially, the model is developed by using the Modular Modeling Methodology (MMM). In order to be more amenable to model-based control techniques, the model suffers a simplification and reduction process, becoming linear and time-invariant (SLIT). Hence, different controllers are then designed based on the reduced model, namely, the proportional-derivative (PD), the linear quadratic regulator (LQR), and the linear quadratic Gaussian (LQG). Finally, a comparative analysis is then performed.*

Keywords: *Modular Modelling Methodology, rollover, anti-roll bars, Control, Rota 2030.*

1. INTRODUCTION

The main goals of a vehicle suspension system are to absorb vibrations generated by uneven surfaces and bumps while maintaining contact between the tires and the road and avoiding unsafe situations such as vehicle rollover. To achieve these objectives, the design of a vehicle suspension system involves a compromise between ride comfort and safety, as presented in Falleiros and Colón (2016). In order to avoid rollover, active roll control systems have been introduced to effectively prevent vehicle rollover accidents (Malvezzi *et al.* (2022), Malvezzi and Coelho (2018) and Malvezzi and Coelho (2014)).

One way to prevent rollover is by using anti-roll bars, which intend to enhance the vehicle's roll stability and are commonly employed to increase roll stiffness, as demonstrated in Cronje and Els (2010). In fact, during curves and evasive manoeuvres, lateral load transfer occurs due to body roll motion. A more effective solution, presenting more roll stiffness, is by means of active anti-roll bars (Paes and Colón (2018)). However, the use of anti-roll bars may impact ride comfort when the vehicle encounters uneven road surfaces.

Several studies have examined the advantages of active-roll bars in passenger cars to address this issue. In Gosselin-Brisson *et al.* (2009), an active anti-roll bar is designed for an off-road vehicle. The used model is of half-car type and the controller of the anti-roll bar is designed using linear optimal control with quadratic cost minimization. An active anti-roll bar control could also be seen in Jeon *et al.* (2012) and Sun *et al.* (2018), in which the complete analysis and design of the active anti-roll bar model and structure as the motor and its reduction are assembled inside the sway bar. A more detailed model of the anti-roll bar is obtained in Paes and Colón (2018), where a more realistic geometrical form is adopted (U-type anti-roll bar) which is also flexible. A Finite Element Model (FEM) is obtained for the bar and the rest of the vehicle is modelled as a half-car, as in the above-mentioned articles. Robust H-Infinity and LQG/LTR controllers are designed for an active anti-roll bar, and simulations are performed for standard manoeuvres, such as the double-lane change.

Vibration damping can be obtained in several forms, including the passive and active forms. In Bein *et al.* (2012)

several vehicle structural designs with different materials are presented to reduce the disturbance levels and improve ride comfort. Other works, for example, Gáspár *et al.* (2005), combine the anti-roll bar with the brake system in order to prevent rollover. The relation between ride comfort and energy efficiency is worked by Mizuta *et al.* (2010) emphasizing the human vibration sensibility as present in the ISO2631 standard. Other norms are mentioned in Uys *et al.* (2007), such as BS6841, applicable in the United Kingdom, and VDI2057, applicable in Germany. In Falleiros and Colón (2016), a comparative analysis is done among different H-Infinity controllers for an active suspension system in which safety and comfort are differently prioritized. In the case of pickup trucks, achieving good comfort and handling characteristics for both on- and off-road conditions has become increasingly important, as highlighted by Cronje and Els (2010). On the other hand, Danesin *et al.* (2003) presents algorithms that focus on roll stiffness, including its non-linearity and the balance between front and rear, while Hrovat (1988) explores the unsprung mass influence on the ride comfort and handling. Additionally, Tong and Guo (2012) presents an approach that involves designing test signals to simulate real-world road conditions, specifically targeting ride comfort. Finally, Mansfield and Griffin (2000) presents a comprehensive analysis of the vibrations experienced by passengers to provide a better understanding of human comfort inside the vehicle. Their study considers the concept of Weber's Law, which precisely explains human perception.

In this work, a more detailed half-car model is obtained to be used in nonlinear and hardware-in-the-loop (HIL) simulations. Initially, the model is developed by using the Modular Modeling Methodology (MMM). In order to be more amenable to model-based control techniques, the model suffers a simplification and reduction process, becoming linear and time-invariant (SLIT). Hence, different controllers are then designed based on the reduced model, namely, the proportional-derivative (PD), the linear quadratic regulator (LQR), and the linear quadratic Gaussian (LQG). A comparative analysis is then performed. The current paper is divided into three parts: first, the development of the half-car model by using the MMM methodology, described in section 2. second, the control designs, presented in section 3. and third, the simulation of the closed-loop nonlinear system applied in the MMM model, shown in section 4. Finally, conclusions and suggestions for future works are drawn in section 5.

2. HALF-CAR MODELING

Considering the inherent complexity of vehicle systems, traditionally, alternative models are preferred in order to design and simulate a car's suspension system, such as the quarter-car model, the half-car model and even a complete model with reduced degrees of freedom. Half-car models that include the presence of anti-roll bars can incorporate different levels of complexity (Paes and Colón (2018); Cronje and Els (2010)).

In this work, the model of a half-car with an anti-roll bar is developed in such a way, that it allows the analyst to include a variety of elements and effects in a modular fashion. In fact, the methodology employed here can be regarded as unique and distinct in comparison with the approaches normally found in the literature.

Several methodologies for obtaining the mathematical models of a constrained set of rigid bodies can be employed, such as those based on the Euler-Lagrange (Meirovitch (2010); Lanczos (2012)) and the Gibbs-Appell (Baruh (1999)) formulations. A comparison between those techniques is found in Desloge (1988). Other methodologies for obtaining the model could be applied, such as the one presented in Colón (2018); Colón (2014); Colón (2015); Colón (2015) based on the Newton-Euler formulation.

The Modular Modeling Methodology (MMM), proposed in Orsino and Hess-Coelho (2015); Orsino (2017) to model multi-body systems and extended to analyze parallel mechanisms in Hess-Coelho *et al.* (2021), is applied here. Figure 1 presents the model schematic diagram and modelling hierarchy. Figures 1 (a) and (b) show the base model adopted and the half-car model. Figure 1 (c) shows the modelling hierarchy adopted with the i-th base model ($i = 1, 2, \ldots, 13$) at the lowest level, the $\mathcal{K}_j$ subsystem ($j = 1, 2, \ldots, 6$) at the intermediate levels, and the system $\mathcal{M}$ at the final level referring to the complete model.

Let $\boldsymbol{q}_i = [y_i, z_i, \phi_i]^{\mathsf{T}}$ be the column-vector of generalized coordinates associated with the motion of the i-th base model on the vertical plane, with y_i and z_i as the horizontal and vertical coordinates of the body-fixed frame, respectively, and ϕ_i being the associated roll angle, definite positive in the counter-clockwise sense. The dynamic model of the base can be written in the following canonical form:

$$\mathbf{M}_i(\boldsymbol{q}_i)\,\ddot{\boldsymbol{q}}_i + \boldsymbol{v}_i(\boldsymbol{q}_i, \dot{\boldsymbol{q}}_i) + \boldsymbol{g}_i(\boldsymbol{q}_i) = \boldsymbol{\tau}_i(\boldsymbol{q}_i) \Leftrightarrow \mathbf{M}_i(\boldsymbol{q}_i)\,\ddot{\boldsymbol{q}}_i = \boldsymbol{f}_i(\boldsymbol{q}_i)\,, \tag{1}$$

where $\mathbf{M}_i$ is the generalized inertia matrix, $\boldsymbol{v}_i$ and $\boldsymbol{g}_i$ are the column-vectors of centrifugal/Coriolis effects and gravitational forces, respectively, $\boldsymbol{\tau}_i$ is the column-vector of input forces used to model the anti-roll bar moment and damper forces, and $\boldsymbol{f}_i = \boldsymbol{\tau}_i - \boldsymbol{v}_i(\boldsymbol{q}_i, \dot{\boldsymbol{q}}_i) - \boldsymbol{g}_i(\boldsymbol{q}_i)$. Additionally, the terms of Eq. (1) are collected below:

$$
\begin{aligned}
\mathbf{M}_i &= \begin{bmatrix} m_i & 0 & -m_i\left(z_{\mathrm{G}_i}c_{\phi_i} + y_{\mathrm{G}_i}s_{\phi_i}\right) \\ 0 & m_i & m_i\left(y_{\mathrm{G}_i}c_{\phi_i} - z_{\mathrm{G}_i}s_{\phi_i}\right) \\ -m_i\left(z_{\mathrm{G}_i}c_{\phi_i} - y_{\mathrm{G}_i}s_{\phi_i}\right) & m_i\left(y_{\mathrm{G}_i}c_{\phi_i} - z_{\mathrm{G}_i}s_{\phi_i}\right) & m_i\left(y_{\mathrm{G}_i}^2 + z_{\mathrm{G}_i}^2\right) + I_i \end{bmatrix}, \\
\boldsymbol{v}_i &= \begin{bmatrix} -m_i\dot{\phi}_i^2\left(y_{\mathrm{G}_i}c_{\phi_i} - z_{\mathrm{G}_i}s_{\phi_i}\right) \\ -m_i\dot{\phi}_i^2\left(z_{\mathrm{G}_i}c_{\phi_i} + y_{\mathrm{G}_i}s_{\phi_i}\right) \\ 0 \end{bmatrix}, \\
\boldsymbol{g}_i &= \begin{bmatrix} 0 \\ m_i g \\ m_i g\left(y_{\mathrm{G}_i}c_{\phi_i} - z_{\mathrm{G}_i}s_{\phi_i}\right) \end{bmatrix}, \\
\boldsymbol{\tau}_i &= \left[f_{\mathrm{Y},i}, f_{\mathrm{Z},i}, \tau_{\mathrm{X},i}\right]^{\mathsf{T}},
\end{aligned}
\tag{2}
$$

where m_i is the mass, I_i is the moment of inertia, y_{G_i} and z_{G_i} are the coordinates of the centre of gravity in the respective body-fixed frame, g is the acceleration of gravity, $f_{\mathrm{Y},i}$, $f_{\mathrm{Z},i}$ and $\tau_{\mathrm{X},i}$ are the forces and moment components of the column-vector of input forces while $c_{\phi_i} = \cos\left(\phi_i\right)$ and $s_{\phi_i} = \sin\left(\phi_i\right)$. The constraints are obtained based on the kinematics and joints centre position on the Earth-fixed frame, as shown in Eq. (3):

$$
\boldsymbol{h}\left(\boldsymbol{q}\right) = \begin{bmatrix}
\boldsymbol{p}_{\mathrm{B}_1}^{\mathsf{I}} - \boldsymbol{p}_{\mathtt{SD},1}^{\mathsf{I}} \\
\phi_1 - \phi_{\mathtt{SD},1} \\
\boldsymbol{p}_{\mathrm{B}_2}^{\mathsf{I}} - \boldsymbol{p}_{\mathrm{FT}_1}^{\mathsf{I}} \\
\boldsymbol{p}_{\mathrm{C}_3}^{3}\left(2\right) - \boldsymbol{p}_{\mathrm{C}_2}^{2}\left(2\right) \\
\phi_3 - \phi_2 \\
\boldsymbol{p}_{\mathrm{T}_3}^{\mathsf{I}} - \boldsymbol{p}_{\mathrm{LT}_{13}}^{\mathsf{I}} \\
\boldsymbol{p}_{\mathrm{B}_4}^{\mathsf{I}} - \boldsymbol{p}_{\mathrm{FB}_1}^{\mathsf{I}} \\
\boldsymbol{p}_{\mathrm{T}_4}^{\mathsf{I}} - \boldsymbol{p}_{\mathrm{LB}_{13}}^{\mathsf{I}} \\
\boldsymbol{p}_{\mathrm{B}_5}^{\mathsf{I}} - \boldsymbol{p}_{\mathrm{C}_2}^{\mathsf{I}} \\
\boldsymbol{p}_{\mathrm{T}_5}^{5}\left(1\right) - \boldsymbol{p}_{\mathrm{B}_6}^{6}\left(1\right) \\
\boldsymbol{p}_{\mathrm{F}_6}^{6}\left(2\right) - \boldsymbol{p}_{\mathrm{BL}_{13}}^{13}\left(2\right) \\
\boldsymbol{p}_{\mathrm{B}_7}^{\mathsf{I}} - \boldsymbol{p}_{\mathtt{SD},7}^{\mathsf{I}} \\
\phi_7 - \phi_{\mathtt{SD},7} \\
\boldsymbol{p}_{\mathrm{T}_8}^{\mathsf{I}} - \boldsymbol{p}_{\mathrm{FT}_7}^{\mathsf{I}} \\
\boldsymbol{p}_{\mathrm{C}_9}^{9}\left(2\right) - \boldsymbol{p}_{\mathrm{C}_8}^{8}\left(2\right) \\
\phi_9 - \phi_8 \\
\boldsymbol{p}_{\mathrm{B}_9}^{\mathsf{I}} - \boldsymbol{p}_{\mathrm{RT}_{13}}^{\mathsf{I}} \\
\boldsymbol{p}_{\mathrm{T}_{10}}^{\mathsf{I}} - \boldsymbol{p}_{\mathrm{FB}_7}^{\mathsf{I}} \\
\boldsymbol{p}_{\mathrm{B}_{10}}^{\mathsf{I}} - \boldsymbol{p}_{\mathrm{RB}_{13}}^{\mathsf{I}} \\
\boldsymbol{p}_{\mathrm{T}_{11}}^{\mathsf{I}} - \boldsymbol{p}_{\mathrm{C}_8}^{\mathsf{I}} \\
\boldsymbol{p}_{\mathrm{B}_{11}}^{11}\left(1\right) - \boldsymbol{p}_{\mathrm{T}_{12}}^{12}\left(1\right) \\
\boldsymbol{p}_{\mathrm{F}_{12}}^{12}\left(2\right) - \boldsymbol{p}_{\mathrm{BR}_{13}}^{13}\left(2\right) \\
\boldsymbol{p}_{\mathrm{T}_6}^{\mathsf{I}} - \boldsymbol{p}_{\mathrm{B}_{12}}^{\mathsf{I}} \\
\phi_6 - \phi_{12}
\end{bmatrix} = \mathbf{0},
\tag{3}
$$

where the points B_i, T_i, C_i, LB_i, LT_i, RB_i, RT_i, FB_i, FT_i, RB_i, RT_i, LB_i, BL_i are associated with the joints location on the i-th body. Let $\boldsymbol{q} = \left[\boldsymbol{q}_1^{\mathsf{T}}, \boldsymbol{q}_2^{\mathsf{T}}, \ldots, \boldsymbol{q}_{13}^{\mathsf{T}}\right]^{\mathsf{T}}$, $\boldsymbol{v} = \dot{\boldsymbol{q}}$ and $\boldsymbol{a} = \dot{\boldsymbol{v}} = \ddot{\boldsymbol{q}}$ be the column-vectors of generalized coordinates, quasi-velocities and quasi-accelerations, respectively. The second time-derivative of Eq. (3) can be written as:

$$
\ddot{\boldsymbol{h}}\left(\boldsymbol{a}, \boldsymbol{v}, \boldsymbol{q}\right) \Leftrightarrow \mathbf{A}\left(\boldsymbol{q}\right)\boldsymbol{a} - \boldsymbol{b}\left(\boldsymbol{v}, \boldsymbol{q}\right) = \mathbf{0},
\tag{4}
$$

where $\mathbf{A}$ is the Jacobian matrix of the constraints and $\boldsymbol{b}$ is a column-vectors of velocity and position-dependent constraints terms. To attenuate the drift during numerical integration, the differential constraints are rewritten as follows:

$$
\mathbf{A}\boldsymbol{a} = \boldsymbol{b} - 2\alpha_{\mathtt{B}}\dot{\boldsymbol{h}} - \beta_{\mathtt{B}}^2\boldsymbol{h},
\tag{5}
$$

where $\alpha_{\mathtt{B}} > 0$ and $\beta_{\mathtt{B}} > 0$ are stabilizing constants. In the absence of constraints, $\boldsymbol{a}_0 = \mathbf{M}^{-1}\boldsymbol{f}$ is the column-vector of quasi-accelerations, with $\mathbf{M}$ and $\boldsymbol{f}$ as the generalized inertia matrix and column-vector of active forces of the relaxed model, respectively, given by:

$$
\mathbf{M} = \mathrm{blkdiag}\left(\mathbf{M}_1, \mathbf{M}_2, \ldots, \mathbf{M}_{13}\right); \quad \boldsymbol{f} = \left[\boldsymbol{f}_1^{\mathsf{T}}, \boldsymbol{f}_2^{\mathsf{T}}, \ldots, \boldsymbol{f}_{13}^{\mathsf{T}}\right]^{\mathsf{T}}.
\tag{6}
$$

The constraints are imposed based on the relaxed model of Eq. (6) and the differential constraints of Eq. (5) using the Udwadia-Kalaba equation, as follows:

$$
\boldsymbol{a} = \boldsymbol{a}_0 + \mathbf{M}^{-1}\mathbf{A}^{\mathsf{T}}\left(\mathbf{A}\mathbf{M}^{-1}\mathbf{A}^{\mathsf{T}}\right)^{\mathrm{g}}\left(\boldsymbol{b} - 2\alpha_{\mathtt{B}}\dot{\boldsymbol{h}} - \beta_{\mathtt{B}}^2\boldsymbol{h} - \mathbf{A}\boldsymbol{a}_0\right),
\tag{7}
$$

where "g" stands for the generalized inverse.

3. CONTROLLER DESIGN

In order to obtain a mathematical model that can be used in the design of a Linear Time-Invariant (LIT) controller, a simplified model, preferably SLIT, must be obtained. A first simplification of the model presented in section 2is the model represented in Fig. 2.

On the other hand, this model is not yet a LIT model due to gravity acceleration. If this is not included, the state-space equation in continuous time assumes the LIT form:

$$\begin{aligned} \dot{\mathbf{X}}_{\text{SS}} &= \mathbf{A}_{\text{SS}}\mathbf{X}_{\text{SS}} + \mathbf{B}_{\text{SS}}\mathbf{U}_{\text{SS}} + \mathbf{E}_{\text{SS}}, \\ \mathbf{Y}_{\text{SS}} &= \mathbf{C}_{\text{SS}}\mathbf{X}_{\text{SS}}, \end{aligned} \tag{8}$$

where

- $\mathbf{X}_{\text{SS}} = \left[z_1, z_7, z_{13}, \phi_{13}, \dot{z}_1, \dot{z}_7, \dot{z}_{13}, \dot{\phi}_{13}\right]^{\mathsf{T}}$ is the state column-vector,
- $\mathbf{U}_{\text{SS}} = \tau$ is the control input associated with the motor torque of the active anti-roll bar,
- $\mathbf{Y}_{\text{SS}} = \left[\phi_{13}, \dot{\phi}_{13}\right]^{\mathsf{T}}$ is the output column-vector while
- $\mathbf{A}_{\text{SS}}$, $\mathbf{B}_{\text{SS}}$, $\mathbf{E}_{\text{SS}}$ and $\mathbf{C}_{\text{SS}}$ are the state matrices and associated vector, given by:

$$\mathbf{A}_{\text{SS}} = \begin{bmatrix} 0 & 0 & 0 & 0 & 1 & 0 & 0 & 0 \\ 0 & 0 & 0 & 0 & 0 & 1 & 0 & 0 \\ 0 & 0 & 0 & 0 & 0 & 0 & 1 & 0 \\ 0 & 0 & 0 & 0 & 0 & 0 & 0 & 1 \\ -\dfrac{k_{\text{D}}+k_{\text{T}}}{m_1} & 0 & \dfrac{k_{\text{D}}}{m_1} & -\dfrac{k_{\text{D}}\,l}{m_1} & -\dfrac{b_{\text{D}}}{m_1} & 0 & \dfrac{b_{\text{D}}}{m_1} & -\dfrac{b_{\text{D}}l}{m_1} \\ 0 & -\dfrac{k_{\text{D}}+k_{\text{T}}}{m_7} & \dfrac{k_{\text{D}}}{m_7} & \dfrac{k_{\text{D}}l}{m_7} & 0 & -\dfrac{b_{\text{D}}}{m_7} & \dfrac{b_{\text{D}}}{m_7} & \dfrac{b_{\text{D}}l}{m_7} \\ \dfrac{k_{\text{D}}}{m_{13}} & \dfrac{k_{\text{D}}}{m_{13}} & -\dfrac{2k_{\text{D}}}{m_{13}} & 0 & \dfrac{b_{\text{D}}}{m_{13}} & \dfrac{b_{\text{D}}}{m_{13}} & -\dfrac{2b_{\text{D}}}{m_{13}} & 0 \\ -\dfrac{k_{\text{D}}l}{I_{13}} & \dfrac{k_{\text{D}}l}{I_{13}} & 0 & -\dfrac{2k_{\text{D}}l^2+m_{13}gz_{\text{G}_{13}}}{I_{13}} & -\dfrac{b_{\text{D}}l}{I_{13}} & \dfrac{b_{\text{D}}l}{I_{13}} & 0 & -\dfrac{2b_{\text{D}}l^2}{I_{13}} \end{bmatrix}, \tag{9}$$

$$\mathbf{B}_{\text{SS}} = \begin{bmatrix} 0 & 0 & 0 \\ 0 & 0 & 0 \\ 0 & 0 & 0 \\ 0 & 0 & 0 \\ 0 & \dfrac{k_{\text{D}}}{m_1} & 0 \\ 0 & 0 & \dfrac{k_{\text{D}}}{m_7} \\ 0 & 0 & 0 \\ -\dfrac{r_{\text{B}}}{I_{13}} & 0 & 0 \end{bmatrix}; \quad \mathbf{E}_{\text{SS}} = \begin{bmatrix} 0 \\ 0 \\ 0 \\ 0 \\ -\dfrac{m_1 g + k_{\text{D}} l_{\text{D},0} - k_{\text{T}} l_{\text{T},0}}{m_1} \\ -\dfrac{m_7 g + k_{\text{D}} l_{\text{D},0} - k_{\text{T}} l_{\text{T},0}}{m_7} \\ -\dfrac{m_{13} g - 2k_{\text{D}} l_{\text{D},0}}{m_{13}} \\ 0 \end{bmatrix}; \quad \mathbf{C}_{\text{SS}} = \begin{bmatrix} 0 & 0 & 0 & 1 & 0 & 0 & 0 & 0 \\ 0 & 0 & 0 & 0 & 0 & 0 & 0 & 1 \end{bmatrix}.$$

where m_1, m_7 and m_{13} are the mass parameters, I_{13} is the inertia moment, k_{D} and c_{D} are the stiffness and damping coefficients of the suspension, respectively, k_{T} is the stiffness of the tires, r_{D} is the transmission ration between the electric motor of the active anti-roll bar and roll moment on the unsprung mass, which is determined based on the bar parameters and suspension geometry, while $l_{\text{D},0}$ and $l_{\text{T},0}$ are the naturals lengths associated to the suspension spring and tire geometry, in this order.

We should note from Eq. (9) that $l_{\text{D},0}$ and $l_{\text{T},0}$ can be solved in order to make $\mathbf{E}_{\text{SS}} = \mathbf{0}$, thus, compensating for the weight forces in the model. This detail is not present in most half-car models and represents a contribution to the field once it explicitly indicates how the gravity forces are compensated. The model parameters are presented in Table 1.

There are many controls techniques applied in the half-car model like PD, PI, PID and Linear Quadratic Regulator (LQR) Varga *et al.* (2013) while LQG and LQG/LTR can be seen in Sename *et al.* (2019). In this paper, we chose three of them to test: PD, LQR and LQG. The specific details of the control formulation for these techniques can be seen in Ogata (2010), Kirk (2004) and Skogestad and Postlethwaite (2005). The control parameters used are shown in Tab. 2.

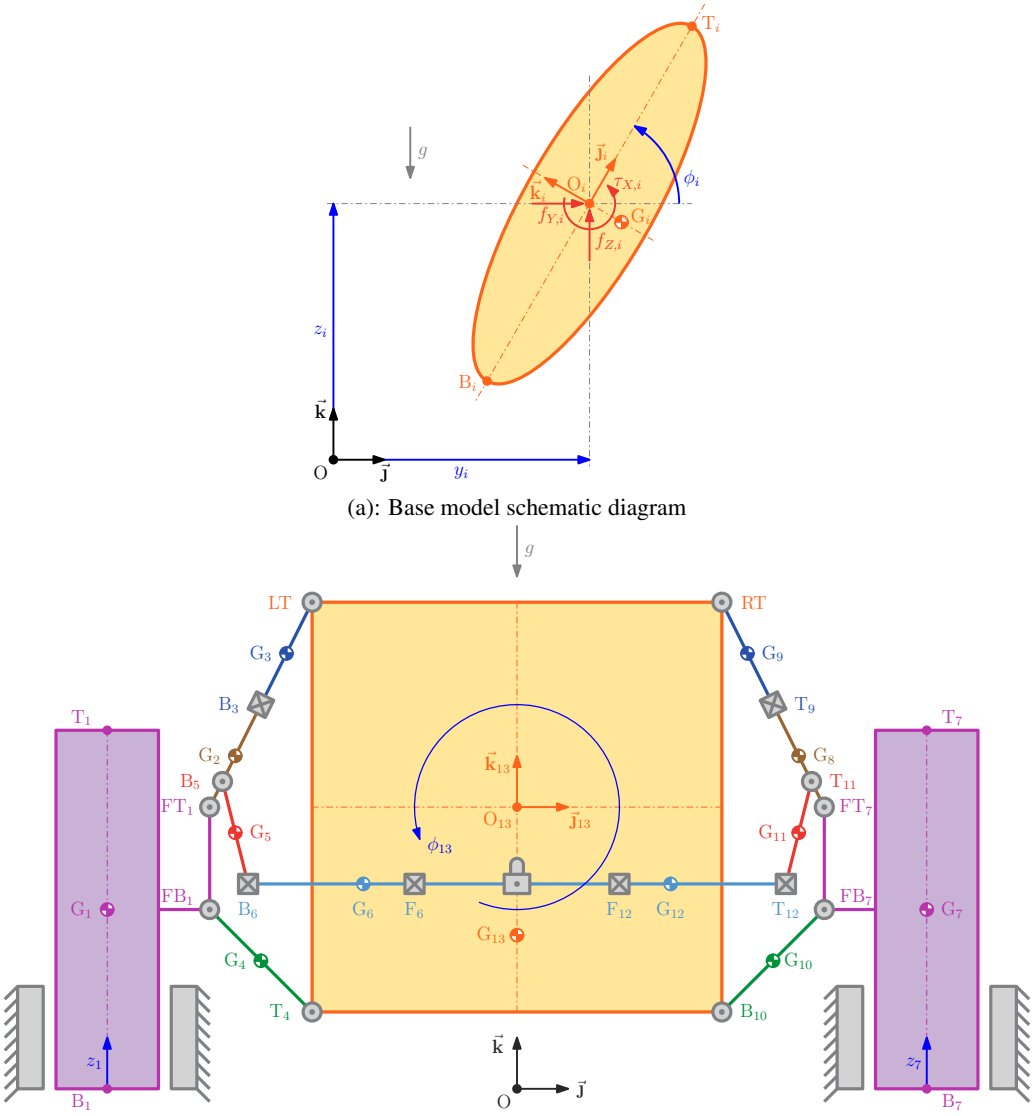

(a): Base model schematic diagram

(b): Half-car model schematic diagram

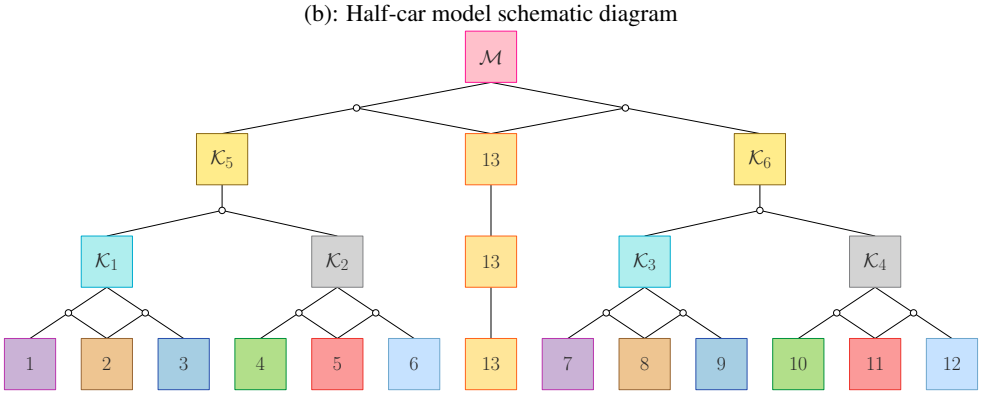

(c): Modeling hierarchy

Figure 1. Half-car model schematic diagram and modeling hierarchy

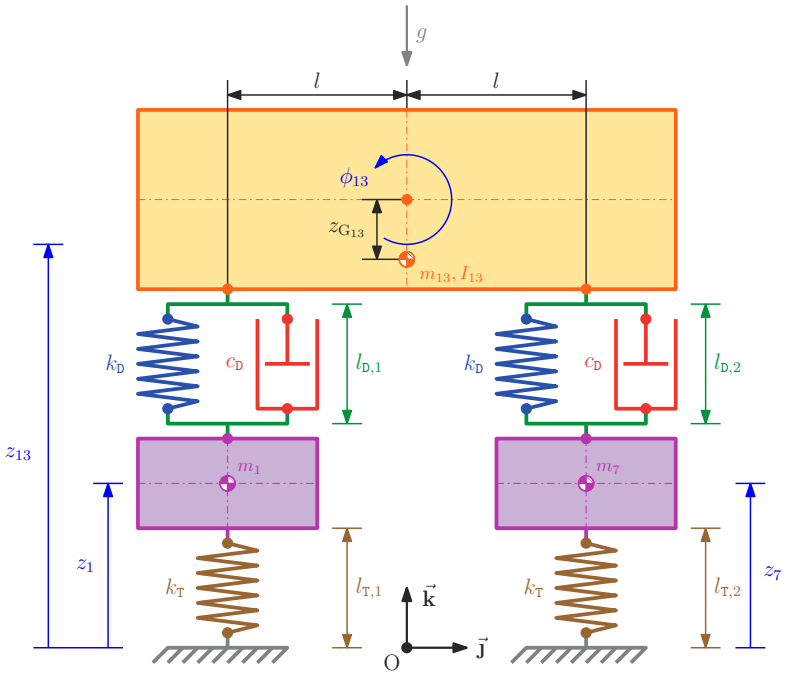

Figure 2. Half-car simplified model

Table 1. Model parameters.

Parameters (Symbols)	**Values**	**Units**
Unsprung mass (m_{13})	528.5	kg
Wheel structure mass (m_1 e m_7)	90	kg
Unsprung inertia moment (I_{13})	417.4	Nm
Suspension damping (c_D)	1000	N/m
Distance from CG to the origin ($z_{G_{13}}$)	0.870	m
Suspension stiffness (k_D)	15000	N/m
Tire stiffness (k_B)	150000	N/m
Length of anti-roll bar arm	0.35	m
Height of anti-roll bar from the ground	0.2	m

Table 2. Control parameters.

Parameters (Symbols)	**Values**	**Units**
Proportional gain (k_P)	2000	–
Derivative gain (k_D)	200	–
States weighting matrix ($\mathbf{Q}$)	$\text{diag}\left(0, 0, 0, 10^6, 0, 0, 0, 10^5\right)$	–
Control weight (R)	10^{-3}	–
States covariance matrix ($\mathbf{Q}_W$)	$\text{diag}\left(5, 5, 5, 7, 5, 5, 5, 7\right)$	–
Measurements covariance matrix ($\mathbf{R}_V$)	$\text{diag}\left(10^{-6}, 10^{-6}\right)$	–

4. RESULTS

The simulation scenario consists of an experiment to induce vehicle rolling by applying periodic displacements on the tires. The displacements are described by a sinusoidal function with an amplitude of 0.1 m and frequency of 2π rad/s. The open-loop and passive response, i.e., using the passive anti-roll bar, are compared to the performance of three standard controllers: PD, LQR and LQG. The simulations were performed in MATLAB/Simulink environment using the ode5 with a fixed time step of 0.001 s.

Figure 3 shows the control results.

As can be seen in Fig. 3 (a) and (b), the LQR and LQG performed well in attenuating the vehicle rolling during the experiment. A smaller oscillation amplitude is achieved with LQG through the tuning of the covariances matrices.

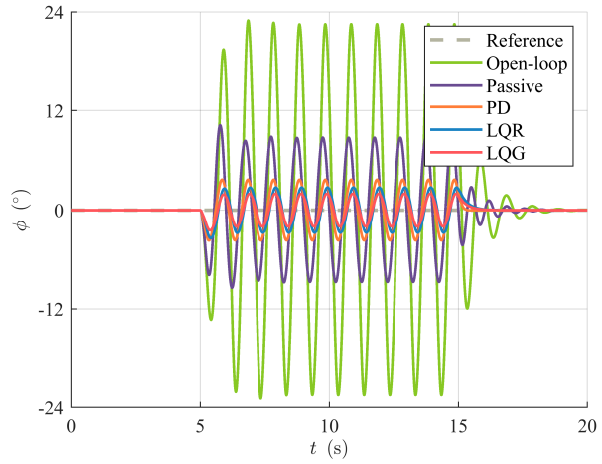

(a): Roll angle

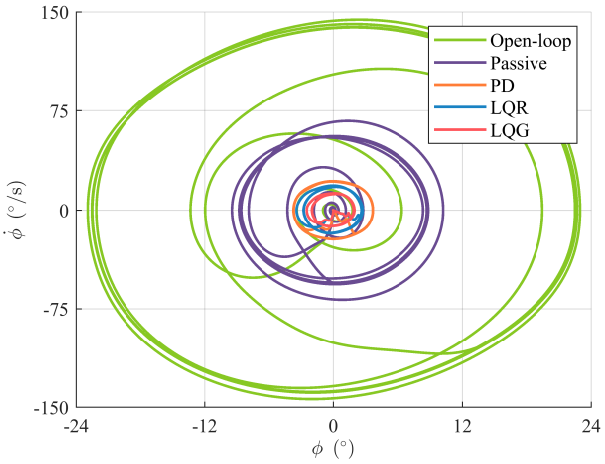

(b): Roll angle phase portrait

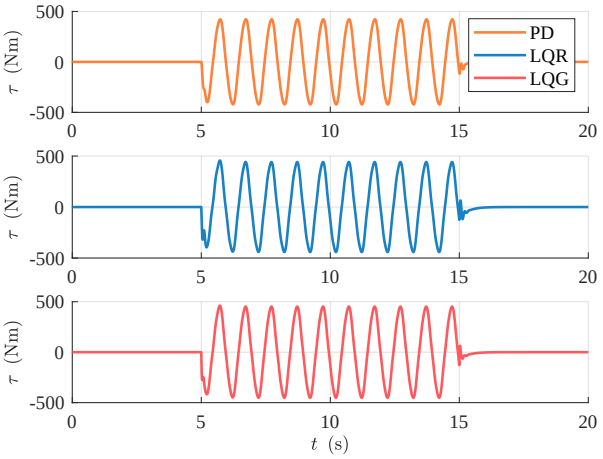

(c): Control torque

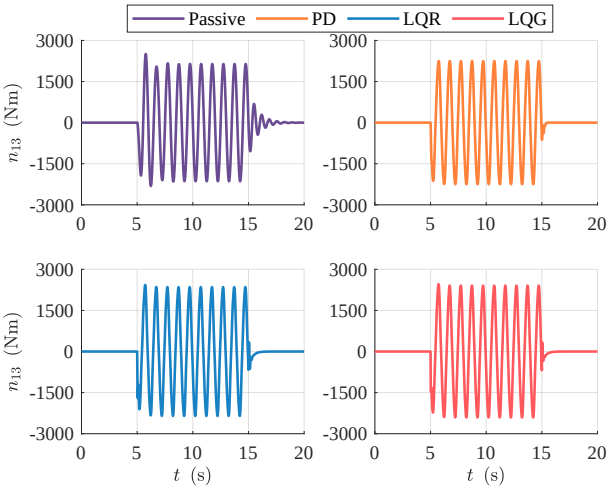

(d): Roll moment

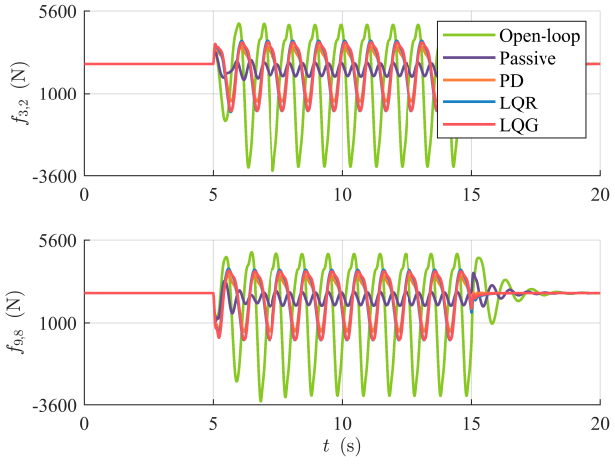

(e): Damper forces

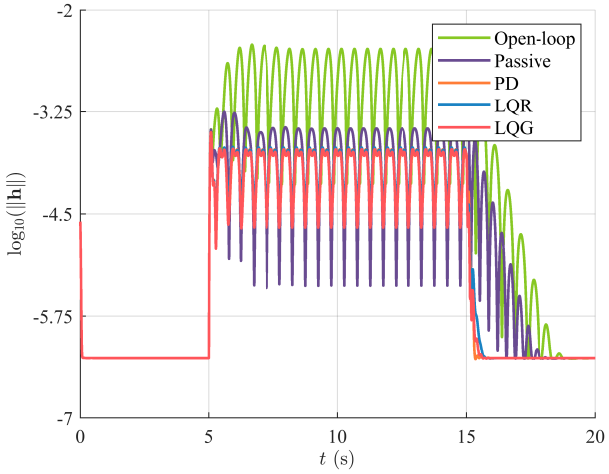

(f): Modeling constraints

Figure 3. Main results

The control inputs are shown in Fig. 3 (c). The amplitude and shape of the motor torque generated by the controllers are similar. The roll moment generated on the unsprung mass shown in Fig. 3 (d) also has a similar behaviour between the active controllers while presenting an undamped profile for the passive anti-roll bar.

Figure 3 (e) shows the damper forces for all the configurations tested. A higher load is imposed on the suspension when the system is either in an open or closed loop in comparison with the passive bar. This effect can be reduced with an integrated suspension control using the dampers and active anti-roll bar together to attenuate the vehicle rolling.

Finally, Fig. 3 (f) shows the order of the constraints of Eq. (3). The order is below 10^{-2} in all the configurations tested, even during the rolling induced by the tire displacements. This small value indicates the consistency in the multibody system modelling.

5. CONCLUSIONS

This paper presented the modelling and control of a passenger vehicle equipped with an active anti-roll bar. A complete half-car model was developed as a multi-body system considering the weight, suspension geometry and anti-roll bar. Also, a simplified and reduced model was formulated to control synthesis taking into account the absolute displacements, weight and the pre-tension associated with the dampers and tires. The simplified model was then used to synthesize the controllers for vehicle rolling, based on the PD, LQR and LQG techniques. Simulation results with the full half-car model revealed the importance of considering the modelling errors and disturbances in the control design. In future works, an integrated suspension control system is intended to be developed to improve performance while reducing the load on the dampers during rolling control. This will be performed considering semi-active electro-hydraulic dampers and an active anti-roll bar composed of an electric motor and gearbox ratio.

6. ACKNOWLEDGEMENTS

Authors would like to acknowledge the Fundação de Desenvolvimento da Pesquisa (FUNDEP) - Rota 2030 - Linha V, for the Grants of the Sistema de Suspensão Semi-Ativa para Controle Avançado de Estabilidade (SUSP-EST)

7. REFERENCES

Baruh, H., 1999. *Analytical dynamics*. McGraw-Hill International Ed edition.

Bein, T., Bös, J., Mayer, D. and Melz, T., 2012. "Advanced materials and technologies for reducing noise, vibration and harshness (nvh) in automobiles". In *Advanced Materials in Automotive Engineering*, Elsevier, pp. 254–298.

Colón, D., 2014. "Connections between screw theory and cartan's connections". In *Proceedings of the Congresso Brasileiro de Automática 2014*. Sociedade Brasileira de Automatica, Belo Horizonte.

Colón, D., 2015. "Cartan's connection, fiber bundles and quaternions in kinematics and dynamics calculations". In *Proceedings of the ASME 2015 IDETC/CIE 2015*. ASME, Boston.

Colón, D., 2018. "Cartan connection applied to dynamic calculation in robotics". *Journal of the Brazilian Society of Mechanical Sciences and Engineering*, Vol. 40, No. 8, p. 369. ISSN 1806-3691.

Colón, D., 2015. "Cartan connections as a tool for kinematic chain calculation". *Journal of Control, Automation and Electrical Systems*, Vol. 26, No. 6, pp. 630–641. ISSN 2195-3899.

Cronje, P.H. and Els, P.S., 2010. "Improving off-road vehicle handling using an active anti-roll bar". *Journal of Terramechanics*, Vol. 47, No. 3, pp. 179–189.

Danesin, D., Krief, P., Sorniotti, A. and Velardocchia, M., 2003. "Active roll control to increase handling and comfort". *SAE transactions*, pp. 1007–1017.

Desloge, E.A., 1988. "The gibbs–appell equations of motion". *American Journal of Physics*, Vol. 56, No. 9, pp. 841–846.

Falleiros, M.F. and Colón, D., 2016. "Lqg/ltr robust active suspension control applied on a nonlinear half-vehicle model". In *Proceedingd of the CBA 2016*.

Gáspár, P., Szaszi, I. and Bokor, J., 2005. "Reconfigurable control structure to prevent the rollover of heavy vehicles". *Control Engineering Practice*, Vol. 13, No. 6, pp. 699–711.

Gosselin-Brisson, S., Bouazara, M. and Richard, M., 2009. "Design of an active anti-roll bar for off-road vehicles". *Shock and Vibration*, Vol. 16, pp. 155–174. doi:10.1155/2009/343048.

Hess-Coelho, T.A., Orsino, R.M.M. and Malvezzi, F., 2021. "Modular modelling methodology applied to the dynamic analysis of parallel mechanisms". *Mechanism and Machine Theory*, Vol. 161, p. 104332. ISSN 0094-114X. doi:https://doi.org/10.1016/j.mechmachtheory.2021.104332. URL `https://www.sciencedirect.com/science/article/pii/S0094114X21000902`.

Hrovat, D., 1988. "Influence of unsprung weight on vehicle ride quality". *Journal of Sound and Vibration*, Vol. 124, No. 3, pp. 497–516.

Jeon, K., Hwang, H., Choi, S., Kim, J., Jang, K. and Yi, K., 2012. "Development of an electric active rollcontrol (arc) algorithm for a suv". *International journal of automotive technology*, Vol. 13, pp. 247–253.

Kirk, D.E., 2004. *Optimal control theory: an introduction*. Courier Corporation.

Lanczos, C., 2012. *The variational principles of mechanics*. Courier Corporation.

Malvezzi, F. and Coelho, T., 2014. "Topological synthesis of a novel parallel mechanism for vehicle rear suspensions". In *New Advances in Mechanisms, Transmissions and Applications: Proceedings of the Second Conference MeTrApp 2013*. Springer, pp. 33–40.

Malvezzi, F. and Coelho, T.A.H., 2018. "Error analysis for an active geometry control suspension system". *Journal of the Brazilian Society of Mechanical Sciences and Engineering*, Vol. 40, pp. 1–25.

Malvezzi, F., Hess Coelho, T.A. and Orsino, R.M.M., 2022. "Feasibility and performance analyses for an active geometry control suspension system for over-actuated vehicles". *Journal of the Brazilian Society of Mechanical Sciences and Engineering*, Vol. 44, No. 5, p. 178.

Mansfield, N.J. and Griffin, M.J., 2000. "Difference thresholds for automobile seat vibration". *Applied Ergonomics*, Vol. 31, No. 3, pp. 255–261.

Meirovitch, L., 2010. *Methods of analytical dynamics*. Courier Corporation.

Mizuta, Y., Suzumura, M. and Matsumoto, S., 2010. "Ride comfort enhancement and energy efficiency using electric active stabiliser system". *Vehicle System Dynamics*, Vol. 48, No. 11, pp. 1305–1323.

Ogata, K., 2010. *Modern control engineering*. Prentice Hall, 5th edition.

Orsino, R.M.M., 2017. "Recursive modular modelling methodology for lumped-parameter dynamic systems". *Proc. R. Soc. A.*, Vol. 473, p. 20160891. doi:10.1098/rspa.2016.0891.

Orsino, R.M.M. and Hess-Coelho, T.A., 2015. "A contribution on the modular modelling of multibody systems". *Proc. R. Soc. A.*, Vol. 471, p. 20150080. doi:10.1098/rspa.2015.0080.

Paes, J.H. and Colón, D., 2018. "Comparison between passive and active flexible anti-roll bars modelles by finite element method on prevention of vehicle rollovers". In *Proceedings of the CBA 2018*.

Sename, O., Dugard, L., Gáspár, P. *et al.*, 2019. "H-infinity/lpv controller design for an active anti-roll bar system of heavy vehicles using parameter dependent weighting functions". *Heliyon*, Vol. 5, No. 6.

Skogestad, S. and Postlethwaite, I., 2005. *Multivariable Feedback Control: Analysis and Design*. Multivariable Feedback Control: Analysis and Design. Wiley. ISBN 9780470011676.

Sun, H., Chen, Y.H., Zhao, H. and Zhen, S., 2018. "Optimal design for robust control parameter for active roll control system: A fuzzy approach". *Journal of Vibration and Control*, Vol. 24, No. 19, pp. 4575–4591.

Tong, W. and Guo, K., 2012. "Simulation testing research on ride comfort of vehicle with global-coupling torsion-elimination suspension". *Physics Procedia*, Vol. 33, pp. 1741–1748.

Uys, P.E., Els, P.S. and Thoresson, M., 2007. "Suspension settings for optimal ride comfort of off-road vehicles travelling on roads with different roughness and speeds". *Journal of Terramechanics*, Vol. 44, No. 2, pp. 163–175.

Varga, B., Németh, B. and Gáspár, P., 2013. "Control design of anti-roll bar actuator based on constrained lq method". In *2013 IEEE 14th International Symposium on Computational Intelligence and Informatics (CINTI)*. IEEE, pp. 31–36.

8. RESPONSIBILITY NOTICE

The authors are solely responsible for the printed material included in this paper.